

Prompt Upsilon and Psi Production at LEP

Peter Cho¹

Lauritsen Laboratory
California Institute of Technology
Pasadena, CA 91125

Abstract

Color-octet contributions to quarkonia production at LEP are studied herein. The short distance formation of heavy quark-antiquark pairs in color-octet configurations via gluon fragmentation processes is significantly enhanced relative to the creation of color-singlet pairs via heavy quark fragmentation. But the subsequent long distance hadronization of these colored pairs into physical quarkonium bound states is suppressed compared to the nonperturbative evolution of their colorless counterparts. We find that the overall LEP rates for gluon fragmentation into prompt Upsilon and Psi vector bosons exceed those from heavy quark fragmentation. Inclusion of the dominant color-octet quarkonium production channel eliminates sizable discrepancies between previous predictions and recent measurements of prompt $Z \rightarrow J/\psi + X$, $Z \rightarrow \psi' + X$ and $Z \rightarrow \Upsilon + X$ branching fractions.

¹ Work supported in part by a DuBridge Fellowship and by the U.S. Dept. of Energy under DOE Grant no. DE-FG03-92-ER40701.

2. Lowest order color-octet quarkonia production

Quarkonia production at LEP involves several different length scales. The first is set by the Z boson mass M_Z which represents the e^+e^- collider's current operating energy. The second is fixed by the mass M_Q of the quark or antiquark inside a quarkonium state. The heavy constituents are bound together over a distance scale determined by their momentum $M_Q v$, and they interact with each other over time periods set by their kinetic energy $M_Q v^2$. Since the velocity $v \sim 1/\log M_Q$ of the Q and \bar{Q} inside the bound state is small compared to the speed of light, these scales are all widely separated from one another:

$$(M_Q v^2)^2 \ll (M_Q v)^2 \ll M_Q^2 \ll M_Z^2. \quad (2.1)$$

The presence of so many different energy scales complicates the analysis of quarkonium production. But the most important characteristics may be simply distilled within an effective field theory framework called Nonrelativistic Quantum Chromodynamics (NRQCD) which systematically keeps track of the hierarchy in (2.1) [15]. This effective theory is based upon a double power series expansion in the short distance strong interaction fine structure constant α_s and the small velocity parameter v . We will work throughout this paper within the NRQCD framework.

To begin, we consider the decay mode

$$Z \rightarrow g + Q\bar{Q}[{}^{2s+1}L_J^{(8)}] \quad (2.2)$$

which creates a colored heavy quark-antiquark pair recoiling against a hard gluon. The lowest order diagrams that mediate this transition are illustrated in fig. 1. The spin, orbital and total angular momentum quantum numbers of the $Q\bar{Q}$ pair are indicated in spectroscopic notation inside the square brackets in (2.2), and its color is labeled by the octet superscript. Using the projection techniques described in refs. [13,16,17], we can start with the general $Z \rightarrow g + Q + \bar{Q}$ amplitude and pick out terms which correspond to the formation of a $Q\bar{Q}$ pair in a specified partial wave, spin and color state. For example, the short distance production amplitude for a colored $L = 0, S = 1$ pair is given by

$$i\mathcal{A}(Z(k+P) \rightarrow g_a(k) + Q\bar{Q}[{}^3S_1^{(8)}]_b(P))_{\text{short}} = \frac{2g_2g_3}{\cos\theta_w} \frac{M}{(M_Z^2 - M^2)} T_3 \delta_{ab} \epsilon^{\mu\nu\sigma\tau} \varepsilon_\mu(k)^* \varepsilon_\nu(P)^* \varepsilon_\sigma(k+P) k_\tau. \quad (2.3)$$

Here $M = 2M_Q$ represents the pair's mass, g_2 and g_3 denote the $SU(2)_L$ and $SU(3)_C$ gauge couplings, T_3 stands for the third weak isospin eigenvalue and θ_w equals the weak mixing angle. The outgoing Q and \bar{Q} in fig. 1 propagate nearly on-shell with a combined momentum P . But the intermediate heavy quark or antiquark line which attaches to the decaying Z is off-shell by an amount of $O(M_Z^2)$. As we shall see, the intermediate particle's extreme virtuality strongly suppresses the lowest order color-octet process in (2.2) relative to quark and gluon fragmentation reactions that take place at higher order in the α_s expansion.

After the colored $Q\bar{Q}[^{2S+1}L_J^{(8)}]$ pair is created within a spacetime interval set by the Z boson mass, it evolves over a much longer time and distance scale into a physical quarkonium bound state. The pair transforms into a colorless hadron via the emission or absorption of one or more soft gluons. These long wavelength gluons bleed off the color of the $Q\bar{Q}[^{2S+1}L_J^{(8)}]$ object, but they carry away only $O(M_Q v^2)$ worth of energy and momentum [15]. In the $M_Q \rightarrow \infty$ limit, this hadronization process should be perturbatively computable. However in the real world where $M_Q v^2 \simeq \Lambda_{QCD}$, the amplitude for a heavy color-octet pair to evolve into a physical quarkonium state is nonperturbative. The long distance matrix element therefore cannot be computed from first principles and must instead be determined from experiment.

Combining together the square of the short distance amplitude in (2.3) with the long distance factor $\mathcal{M}_8(\psi_Q) \equiv |\mathcal{A}(Q\bar{Q}[^3S_1^{(8)}] \rightarrow \psi_Q(n))_{\text{long}}|^2$, we obtain the partial width

$$\Gamma(Z \rightarrow g + Q\bar{Q}[^3S_1^{(8)}] \rightarrow \psi_Q + X) = \frac{\pi}{3} \frac{\alpha_{EM} \alpha_s}{\sin^2 \theta_w \cos^2 \theta_w} \left(\frac{N_c^2 - 1}{2} \right) \left(1 - \frac{M^4}{M_Z^4} \right) \frac{\mathcal{M}_8(\psi_Q)}{M_Z} \quad (2.4)$$

which is averaged (summed) over initial (final) polarizations and colors. The color-octet squared amplitude decomposes into an infinite sum over NRQCD matrix elements

$$\begin{aligned} \mathcal{M}_8(\psi_Q(n)) = \frac{1}{24M_Q} \sum_{m \geq n} \left\{ \langle 0 | \mathcal{O}_8^{\psi_Q(m)}(^3S_1) | 0 \rangle \text{Br}(\psi_Q(m) \rightarrow \psi_Q(n)) \right. \\ \left. + \sum_{J=0,1,2} \langle 0 | \mathcal{O}_8^{\chi_{QJ}(m)}(^3S_1) | 0 \rangle \text{Br}(\chi_{QJ}(m) \rightarrow \psi_Q(n)\gamma) + \dots \right\} \end{aligned} \quad (2.5)$$

which determine the probabilities for a $Q\bar{Q}[^3S_1^{(8)}]$ pair to turn into a ψ_Q through all possible intermediate channels. Numerical values for these NRQCD matrix elements have recently been extracted from CDF Upsilon and Psi cross section measurements in refs. [13,14].

Once the universal matrix elements are known from one experiment, they may be applied to the study of color-octet quarkonia production at any other.

Inserting the long distance squared amplitude values

$$\begin{aligned}
\mathcal{M}_8(J/\psi) &= 6.8 \times 10^{-4} \text{ GeV}^2 \\
\mathcal{M}_8(\psi') &= 2.0 \times 10^{-4} \text{ GeV}^2 \\
\sum_{n=1}^3 \mathcal{M}_8(\Upsilon(nS)) &= 6.4 \times 10^{-3} \text{ GeV}^2
\end{aligned}
\tag{2.6}$$

into (2.4) along with the parameters $M_c = 1.48 \text{ GeV}$, $M_b = 4.88 \text{ GeV}$, $\alpha_s(2M_c) = 0.28$ and $\alpha_s(2M_b) = 0.19$, we find the $Z \rightarrow J/\psi + X$, $Z \rightarrow \psi' + X$, and $Z \rightarrow \sum_n \Upsilon(nS) + X$ branching fractions listed in the first row of Table I. Comparing these predictions with the OPAL numbers in eqns. (1.2) and (1.3), we see that the contribution to Upsilon and Psi production at LEP from the color-octet process in (2.2) with an $L = 0$, $S = 1$ intermediate state is negligible. Yields from similar reactions involving colored $Q\bar{Q}$ pairs with different orbital and spin angular momenta should be even smaller since their hadronization into physical bound states takes place at higher orders in the velocity expansion. We therefore conclude that $O(\alpha_s)$ color-octet quarkonia production channels can be ignored without loss.

3. Heavy quark fragmentation

Parton fragmentation represents the dominant source of heavy quarkonia in high energy collisions [18]. As we have seen, the propagators of short distance intermediate partons are usually off-shell by $O(1/E^2)$ where E denotes some characteristic energy of the hard reaction. But in fragmentation processes, the quark or gluon which splits into a quarkonium state plus other partons is typically off-shell by only $O(1/M_Q^2)$. At sufficiently high energies, fragmentation contributions to quarkonia cross sections dominate over all non-fragmentation competitors since the former are enhanced relative to the latter by powers of E^2/M_Q^2 . This outcome is guaranteed to occur even if the short distance part of the fragmentation reaction takes place at higher order in the α_s expansion, for additional factors of the QCD coupling only logarithmically suppress reaction rates with increasing E .

One of the first applications of these fragmentation ideas was to charmonia and bottomonia production at LEP. In ref. [5], Braaten, Cheung and Yuan calculated the probabilities for charm and bottom quarks to respectively split into Psi and Upsilon bound

states. These authors then folded together the fragmentation probabilities with the $Z \rightarrow c\bar{c}$ and $Z \rightarrow b\bar{b}$ partial widths and determined the prompt quarkonia branching fraction $\text{Br}(Z \rightarrow \psi_Q + X)_{Q \text{ frag}}$. We will review the findings of Braaten *et al.* below and then generalize their color-singlet results to include color-octet contributions as well.

Heavy quark fragmentation production of Upsilon and Psi bosons at LEP proceeds at $O(\alpha_s^2)$ through the Feynman graphs illustrated in fig. 2.¹ The mass s of the virtual heavy quark or antiquark which splits into the outgoing $Q\bar{Q}$ pair ranges over the interval $3M_Q \leq s \leq M_Z - M_Q$. ψ_Q production is maximized when the pair is created near the M_Q scale in a color-singlet $L = 0, S = 1$ configuration. In the fragmentation approximation, the contribution of this channel to the $Z \rightarrow \psi_Q$ partial width simply equals the product of the $Z \rightarrow Q\bar{Q}$ decay rate and the hadronization probabilities $D_{Q \rightarrow \psi_Q}$ and $D_{\bar{Q} \rightarrow \psi_Q}$ [5]:

$$\Gamma(Z \rightarrow Q + \bar{Q} + Q\bar{Q}[{}^3S_1^{(1)}] \rightarrow \psi_Q + X) = \Gamma(Z \rightarrow Q\bar{Q}) \times (D_{Q \rightarrow \psi_Q} + D_{\bar{Q} \rightarrow \psi_Q}) \quad (3.1)$$

where

$$D_{Q \rightarrow \psi_Q} = D_{\bar{Q} \rightarrow \psi_Q} = \frac{8\alpha_s(M)^2}{N_c} \left(\frac{N_c^2 - 1}{2N_c} \right)^2 \left[\frac{1189}{30} - 57 \ln 2 \right] \frac{\mathcal{M}_1(\psi_Q)}{M^2}. \quad (3.2)$$

All nonperturbative information associated with ψ_Q bound state formation resides within the squared amplitude

$$\begin{aligned} \mathcal{M}_1(\psi_Q(n)) &= |\mathcal{A}(Q\bar{Q}[{}^3S_1^{(1)}] \rightarrow \psi_Q(n))_{\text{long}}|^2 \\ &= \frac{1}{6N_c M_Q} \sum_{m \geq n} \left\{ \langle 0 | \mathcal{O}_1^{\psi_Q(m)}({}^3S_1) | 0 \rangle \text{Br}(\psi_Q(m) \rightarrow \psi_Q(n)) + \dots \right\}. \end{aligned} \quad (3.3)$$

Numerical values for the color-singlet NRQCD matrix elements which enter at lowest order in the velocity expansion into this long distance factor can be extracted from the charmonia and bottomonia wavefunctions at the origin tabulated in ref. [19]. Adopting the values

$$\begin{aligned} \mathcal{M}_1(J/\psi) &= 6.1 \times 10^{-2} \text{ GeV}^2 \\ \mathcal{M}_1(\psi') &= 2.9 \times 10^{-2} \text{ GeV}^2 \\ \sum_{n=1}^3 \mathcal{M}_1(\Upsilon(nS)) &= 2.3 \times 10^{-1} \text{ GeV}^2, \end{aligned} \quad (3.4)$$

¹ The two diagrams displayed in fig. 2 dominate in axial gauge over two other $Z \rightarrow \psi_Q Q\bar{Q}$ graphs which do not possess an obvious fragmentation interpretation. Analysis of ψ_Q production via heavy quark fragmentation is most transparent in this particular gauge.

we derive the heavy quark fragmentation branching ratios listed in the second row of Table I.

It is instructive to compare these color-singlet results with their color-octet analogues. The partial width for $Z \rightarrow Q + \bar{Q} + Q\bar{Q}[{}^3S_1^{(8)}] \rightarrow \psi_Q + X$ is readily obtained from $\Gamma(Z \rightarrow Q + \bar{Q} + Q\bar{Q}[{}^3S_1^{(1)}] \rightarrow \psi_Q + X)$ by performing the following color-factor and squared amplitude substitutions in eqn. (3.2):

$$\left(\frac{N_c^2 - 1}{2N_c}\right)^2 \rightarrow \frac{N_c^2 - 1}{4N_c^2} \quad \text{and} \quad \mathcal{M}_1(\psi_Q) \rightarrow \mathcal{M}_8(\psi_Q). \quad (3.5)$$

These alterations diminish both the short and long distance contributions to the color-octet rate relative to its color-singlet counterpart. The color-octet heavy quark fragmentation branching ratios appearing in the third row of Table I are consequently much smaller than their color-singlet counterparts.

Comparing the predicted rates for the processes in eqn. (1.1) with the Upsilon and Psi measurements in eqns. (1.2) and (1.3), we see that heavy quark fragmentation does not appear to account for most prompt quarkonia observed at LEP. Although the data are preliminary and their error bars are large, the sizable mismatch between theory and experiment suggests that other rapid production mechanisms are at work. We therefore turn to consider gluon fragmentation contributions to Upsilon and Psi production in the following section.

4. Gluon fragmentation

A number of striking disagreements between theoretical predictions and experimental measurements of quarkonia cross sections at hadron colliders have arisen during the past few years. The CDF collaboration has discovered that prompt J/ψ and ψ' production at the Tevatron exceed color-singlet differential rate predictions by orders of magnitude [20,21]. CDF has also observed greater numbers of $\Upsilon(1S)$, $\Upsilon(2S)$ and $\Upsilon(3S)$ vector mesons than were originally anticipated [22]. These experimental surprises from Fermilab have stimulated several recent theoretical investigations of quarkonia creation in general and gluon fragmentation processes in particular [7–14]. The incorporation of color-octet production mechanisms into cross section calculations has been demonstrated to yield significantly better descriptions of charmonia and bottomonia measurements than those based upon color-singlet mechanisms alone. Since numerical values for long distance color-octet

matrix elements are *a priori* unknown, the absolute magnitude for $d\sigma(p\bar{p} \rightarrow \psi_Q + X)/dp_\perp$ must simply be fitted to data. But the shapes of the predicted and measured differential distributions at high p_\perp agree quite well once gluon fragmentation reactions are taken into account. Moreover, the fitted values for the color-octet matrix elements are consistent with NRQCD velocity counting rules. Color-octet contributions thus appear to eliminate large discrepancies between theory and experiment.

Given that gluon fragmentation plays a central role in quarkonia production at the Tevatron, it is interesting to study its impact at LEP as well. Gluon fragmentation mediated decays of Z bosons into Upsilon and Psi final states start at $O(\alpha_s^2)$ through the reaction displayed in eqn. (1.4) and illustrated in fig. 3. A straightforward computation yields the differential rate for this process:

$$\begin{aligned} \frac{d^2\Gamma}{dE_1 dE_2}(Z \rightarrow q + \bar{q} + g^* \rightarrow \psi_Q + X) &= \frac{16K}{\delta^2} \left\{ 2(E_1^2 + E_2^2)(1 - 2E_1)(1 - 2E_2) \right. \\ &\quad + \delta^2 [8E_1 E_2 (E_1 + E_2) - 2(3E_1^2 + 4E_1 E_2 + 3E_2^2) + 4(E_1 + E_2) - 1] \\ &\quad \left. + \delta^4 (1 - 2E_1)(1 - 2E_2) \right\} / [(1 - 2E_1)^2 (1 - 2E_2)^2]. \end{aligned} \quad (4.1)$$

Here E_1 and E_2 represent the dimensionless lab frame energies of the quark and antiquark scaled relative to the Z mass, $\delta = M/M_Z$ equals the rescaled quarkonium mass and K denotes a constant prefactor

$$K = \alpha_s^2 \left(\frac{N_c^2 - 1}{2N_c} \right) \Gamma(Z \rightarrow q\bar{q}) \frac{\mathcal{M}_8(\psi_Q)}{M_Z^2} \quad (4.2)$$

which contains the rescaled long distance matrix element $\mathcal{M}_8(\psi_Q)/M_Z^2$. The $O(\delta^2)$ and $O(\delta^4)$ terms inside the curly brackets in (4.1) are negligibly small compared to the leading $O(\delta^0)$ term since $\delta^2 \ll 1$. Similarly, corrections to the $Z \rightarrow q\bar{q}g^*$ partial width from the masses of the q and \bar{q} are unimportant and have been ignored.

Integrating the differential expression in (4.1) over the quark and antiquark energy limits $0 \leq E_1 \leq (1 - \delta^2)/2$ and $(1 - \delta^2)/2 - E_1 \leq E_2 \leq [1 - \delta^2/(1 - 2E_1)]/2$, we obtain the partial decay rate [6]

$$\begin{aligned} \Gamma(Z \rightarrow q + \bar{q} + g^* \rightarrow \psi_Q + X) &= \frac{2K}{\delta^2} \left\{ (1 + \delta^2)^2 \log \delta^2 \log \frac{\delta^2}{(1 + \delta^2)^2} + (3 + 4\delta^2 + 3\delta^4) \log \delta^2 \right. \\ &\quad \left. + 5(1 - \delta^4) + 2(1 + \delta^2)^2 \left[\text{Li}_2\left(\frac{\delta^2}{1 + \delta^2}\right) - \text{Li}_2\left(\frac{1}{1 + \delta^2}\right) \right] \right\}. \end{aligned} \quad (4.3)$$

The $1/\delta^2$ term appearing alongside the constant prefactor K originates from the propagator of the virtual gluon. We again recall that the fragmenting g^* is off-shell by an amount of order M_Q^2 rather than M_Z^2 . The integrated rate for the gluonic process is thus enhanced by the same $1/\delta^2$ factor as its heavy quark fragmentation analogue.

The gluonic channel's rate is further amplified by a large double logarithm. The source of the $(\log \delta^2)^2$ factor appearing in the first term of (4.3) can be traced to the double pole residing in the first term of (4.1). The double log in the integrated rate results from the overlap of an infrared singularity with a collinear divergence. As $\log \delta^2$ is numerically large in both the charmonia and bottomonia sectors, higher order corrections to the gluon fragmentation partial width are likely to be significant. The leading logarithms should be resummed in order to obtain a more reliable estimate for the rate at which ψ_Q quarkonia are generated via gluon fragmentation at LEP. Performing such a resummation is rather subtle, and we will return to this issue in a future work. For now, we will simply evaluate the lowest order expression with the understanding that subleading corrections may not be negligible.

With the extra double log enhancement factor, the short distance contribution to the gluon fragmentation process in (1.4) dominates over that for the heavy quark fragmentation reaction in (1.1). But the long distance color-octet matrix element $\mathcal{M}_8(\psi_Q)$ for the former is numerically two orders of magnitude smaller than the corresponding color-singlet squared amplitude $\mathcal{M}_1(\psi_Q)$ for the latter. The relative importance of these two different fragmentation mechanisms thus depends upon the outcome of a competition between short and long distance factors. To determine the winner, we evaluate the partial width in (4.3) and list the resulting $Z \rightarrow \Upsilon$ and $Z \rightarrow \psi$ branching fractions in the last row of Table I. Comparing these entries with the others in the table, we see that the gluon fragmentation rate beats those for all other prompt quarkonia production channels.

Inclusion of the dominant color-octet contributions brings theoretical branching fraction predictions into line with the experimental values quoted in eqns. (1.2) and (1.3). These results consequently represent a nontrivial success of the color-octet picture. We also note that the rate for gluon fragmentation production of J/ψ is consistent with the L3 upper bound $\text{Br}(Z \rightarrow q\bar{q}g^* \rightarrow J/\psi + X) < 7.0 \times 10^{-4}$ [23] and the more recent DELPHI limit $\text{Br}(Z \rightarrow q\bar{q}g^* \rightarrow J/\psi + X) < 4.1 \times 10^{-4}$ [3]. Improved LEP measurements of this branching ratio along with its ψ' and Υ analogues would provide useful cross checks on NRQCD color-octet matrix element values. Angular distribution and spin alignment data would further test color-octet mechanism ideas. In short, further observation of Z decays to Upsilon and Psi final states would enhance understanding of basic quarkonium physics.

5. Conclusions

In this article, we have investigated color-octet contributions to prompt quarkonia production at LEP.² The quantitative results of our study compiled in Table I can be qualitatively understood by considering the order of magnitude estimates displayed in Table II. In the first column, we list the perturbative QCD order for each of the production channels that we have considered in this paper. We next recall in the second column the short distance factors associated with each mode. As we have seen, the $1/\delta^2 = M_Z^2/M^2$ enhancement of the fragmentation reactions overwhelms their $O(\alpha_s)$ suppression relative to lowest order non-fragmentation processes. Rates for the former consequently swamp those for the latter. The branching fraction for the gluonic mode in (1.4) is further amplified by a large double log. In the third and fourth columns of Table II, we enumerate the relevant color and flavor factors for each of the production channels. It is important to note that these factors enhance the gluon fragmentation mode by an order of magnitude relative to its heavy quark counterpart. Finally, we list the long distance matrix elements associated with each process. An interesting interplay between the various factors appearing in the columns of this table determines the relative importance of the production mechanisms listed in the separate rows.

The nonperturbative suppression of color-octet processes generally implies that they are subdominant compared to color-singlet reactions. Intermediate $b\bar{b}[{}^3S_1^{(8)}]$ and $c\bar{c}[{}^3S_1^{(8)}]$ contributions to bottom and charm quark fragmentation into Upsilon and Psi final states are negligible compared to those from $b\bar{b}[{}^3S_1^{(1)}]$ and $c\bar{c}[{}^3S_1^{(1)}]$ pairs. But in certain circumstances, short distance enhancement of color-octet modes can offset their long distance suppression. A striking example of this phenomenon has recently been proposed as a resolution to the CDF ψ' surplus problem [12]. Short distance enhancement of $g \rightarrow c\bar{c}[{}^3S_1^{(8)}]$ could yield 50 times more high p_\perp ψ' charmonia than $g \rightarrow c\bar{c}[{}^3S_1^{(1)}]$ even though the hadronization rate for colored pairs from the first reaction is suppressed by $O(v^4)$ compared to that for colorless pairs from the second. A similar phenomenon may play an important role at LEP. We have found that inclusion of the dominant gluon fragmentation channel (1.4) removes sizable disparities between previous theoretical predictions and recent experimental measurements of $Z \rightarrow J/\psi + X$, $Z \rightarrow \psi' + X$ and $Z \rightarrow \Upsilon + X$ branching fractions. Color-octet mechanism ideas thus appear to solve puzzles that have been encountered in both hadron and lepton collider settings. Our confidence is therefore

² Similar work has recently been reported by Cheung, Keung and Yuan in ref. [24].

bolstered that these same ideas can be applied to quarkonia problems in other contexts as well.

Acknowledgments

It is a pleasure to thank Stan Brodsky, Howard Georgi, Ian Hinchliffe and Mark Wise for helpful discussions.

Production Mechanism	$\text{Br}(Z \rightarrow J/\psi)$	$\text{Br}(Z \rightarrow \psi')$	$\sum_{n=1}^3 \text{Br}(Z \rightarrow \Upsilon(nS))$
$Z \rightarrow g + Q\bar{Q}[{}^3S_1^{(8)}]$	1.6×10^{-7}	4.6×10^{-8}	1.0×10^{-6}
$Z \rightarrow Q + \bar{Q} + Q\bar{Q}[{}^3S_1^{(1)}]$	7.7×10^{-5}	3.7×10^{-5}	1.6×10^{-5}
$Z \rightarrow Q + \bar{Q} + Q\bar{Q}[{}^3S_1^{(8)}]$	1.1×10^{-7}	3.2×10^{-8}	5.7×10^{-8}
$Z \rightarrow q + \bar{q} + Q\bar{Q}[{}^3S_1^{(8)}]$	3.3×10^{-4}	9.6×10^{-5}	4.1×10^{-5}

Table I

Production Mechanism	QCD Order	Short Distance Factor	Color Factor	Flavor Factor	Long Distance Matrix Element
$Z \rightarrow g + Q\bar{Q}[{}^3S_1^{(8)}]$	α_s	1	$\frac{N_c^2 - 1}{2}$	1	$\mathcal{M}_8(\psi_Q)$
$Z \rightarrow Q + \bar{Q} + Q\bar{Q}[{}^3S_1^{(1)}]$	α_s^2	$\frac{1}{\delta^2}$	$\left(\frac{N_c^2 - 1}{2N_c}\right)^2$	1	$\mathcal{M}_1(\psi_Q)$
$Z \rightarrow Q + \bar{Q} + Q\bar{Q}[{}^3S_1^{(8)}]$	α_s^2	$\frac{1}{\delta^2}$	$\frac{N_c^2 - 1}{4N_c^2}$	1	$\mathcal{M}_8(\psi_Q)$
$Z \rightarrow q + \bar{q} + Q\bar{Q}[{}^3S_1^{(8)}]$	α_s^2	$\frac{(\log \delta^2)^2}{\delta^2}$	$\frac{N_c^2 - 1}{2}$	5	$\mathcal{M}_8(\psi_Q)$

Table II

References

- [1] The OPAL collaboration, “Observation of Υ production in hadronic Z^0 decays, OPAL Physics note PN192, (1995), unpublished.
- [2] The OPAL collaboration, “ J/ψ and ψ' production in hadronic Z^0 decays”, OPAL Physics Note PN178 (1995), unpublished.
- [3] The DELPHI collaboration, “Search for promptly produced heavy quarkonium states in hadronic Z decays”, CERN-PPE/Paper 0116 (1995), unpublished.
- [4] The DELPHI collaboration, Phys. Lett. **B341** (1994) 109.
- [5] E. Braaten, K. Cheung and T.C. Yuan, Phys. Rev. **D48** (1993) 4230.
- [6] K. Hagiwara, A.D. Martin and W.J. Stirling, Phys. Lett. **B267** (1991) 527; (E) Phys. Lett. **B316** (1993) 631.
- [7] E. Braaten and T.C. Yuan, Phys. Rev. **D50** (1994) 3176.
- [8] E. Braaten, M.A. Doncheski, S. Fleming and M.L. Mangano, Phys. Lett. **B333** (1994) 548.
- [9] D.P. Roy and K. Sridhar, Phys. Lett. **B339** (1994) 141.
- [10] M. Cacciari and M. Greco, Phys. Rev. Lett. **73** (1994) 1586.
- [11] P.Cho and M. Wise, Phys. Lett. **B346** (1995) 129.
- [12] E. Braaten and S. Fleming, Phys. Rev. Lett. **74** (1995) 3327.
- [13] P. Cho and A.K. Leibovich, CALT-68-1988 (1995), unpublished.
- [14] M. Cacciari, M. Greco, M.L. Mangano and A. Petrelli, CERN-TH/95-129 (1995), unpublished.
- [15] G.T. Bodwin, E. Braaten and G.P. Lepage, Phys. Rev. **D51** (1995) 1125.
- [16] J. H. Kühn, J. Kaplan and E. G. O. Safiani, Nucl. Phys. **B157** (1979) 125.
- [17] B. Guberina, J.H. Kühn, R.D. Peccei and R. Rückl, Nucl. Phys. **B174** (1980) 317.
- [18] E. Braaten and T.C. Yuan, Phys. Rev. Lett. **71** (1993) 1673.
- [19] E.J. Eichten and C. Quigg, Phys. Rev. **D47** (1995) 1726.
- [20] The CDF collaboration, Fermilab-Conf-94/136-E (1994), unpublished.
- [21] The CDF collaboration, Fermilab-Conf-95/128-E (1995), unpublished.
- [22] The CDF collaboration, Fermilab-Conf-94/221-E (1994), unpublished.
- [23] The L3 collaboration, Phys. Lett. **B288** (1992) 412.
- [24] K. Cheung, W.-Y. Keung and T.C. Yuan, Fermilab-Pub-95/300-T (1995), unpublished.

Figure Captions

- Fig. 1. Feynman diagrams which mediate the lowest order color-octet process $Z \rightarrow g + Q\bar{Q}[{}^{2s+1}L_J^{(8)}] \rightarrow \psi_Q + X$.
- Fig. 2. Feynman diagrams which mediate the heavy quark fragmentation process $Z \rightarrow Q + \bar{Q} + Q\bar{Q}[{}^{2s+1}L_J^{(8)}] \rightarrow \psi_Q + X$. Two other non-fragmentation graphs whose $O(\alpha_s^2)$ contributions are subleading in axial gauge are not pictured.
- Fig. 3. Feynman diagrams which mediate the gluon fragmentation process $Z \rightarrow q + \bar{q} + g^* \rightarrow q + \bar{q} + Q\bar{Q}[{}^3S_1^{(8)}] \rightarrow \psi_Q + X$.

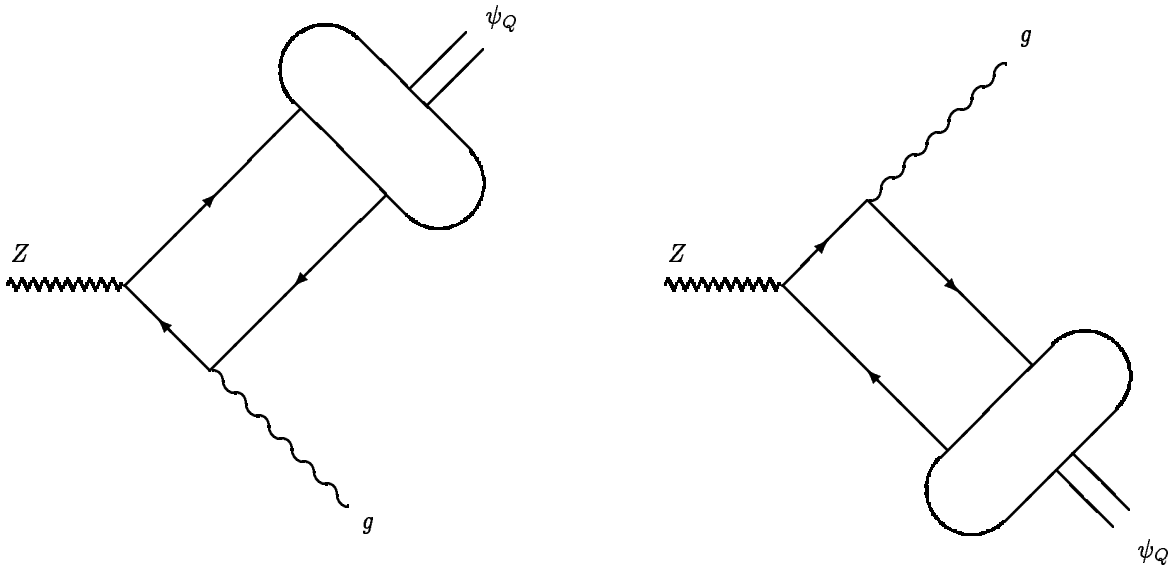


Figure 1

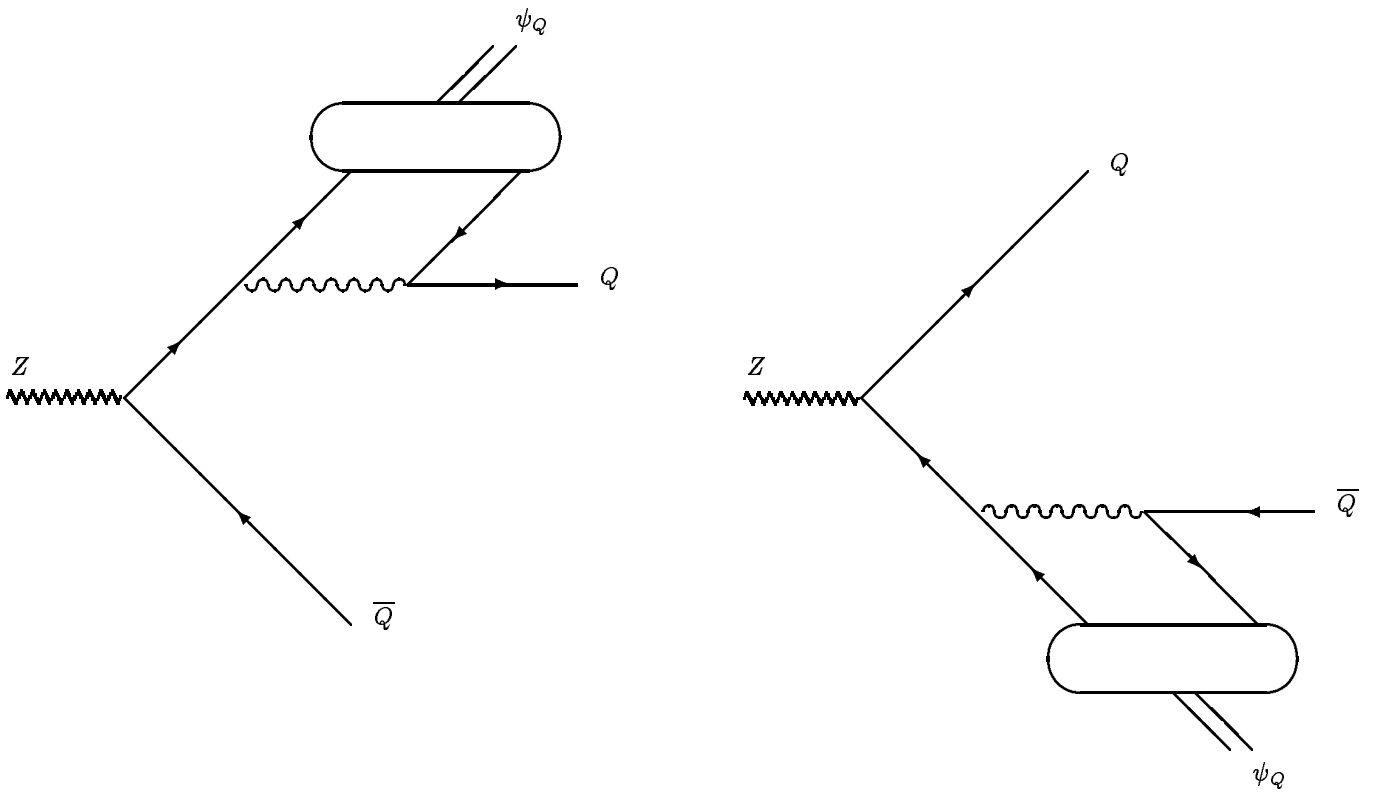


Figure 2

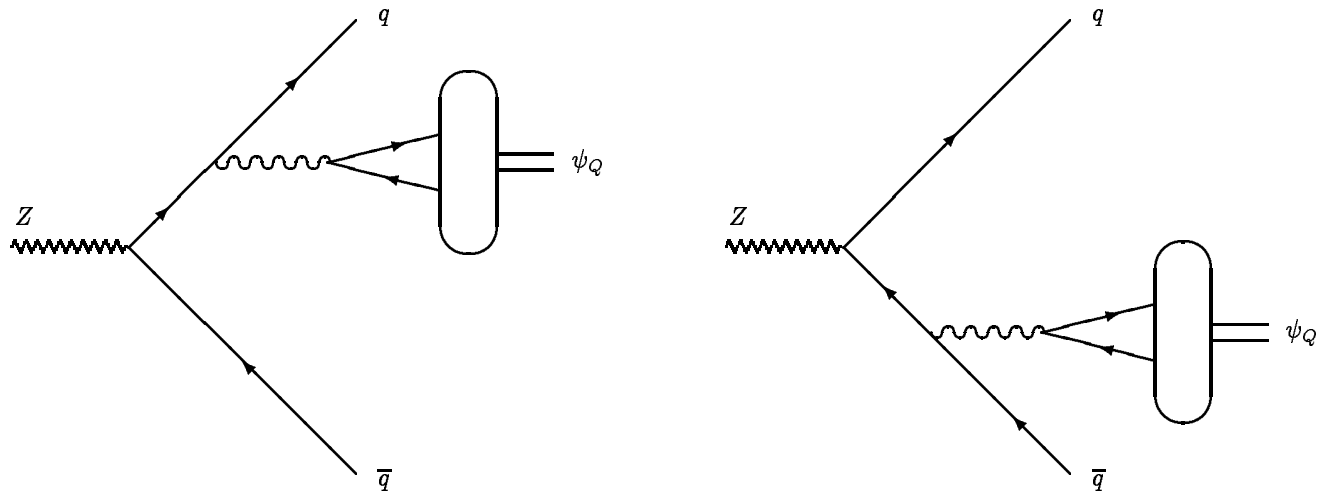


Figure 3